IOCMA 2026 Conference

The 2nd International Online Conference on Mathematics and Applications

10–12 June 2026 | Online

MDPI

Mathematical Modeling and Surface-Based Quantification of Hemodynamics in Abdominal Aortic Aneurysms

Spyridon C. Katsoudas[1], Panagiotis D. Linardopoulos[1], Anastasios A. Raptis[2], Konstantinos G. Moulakakis[3], John D. Kakisis[3], Konstantinos T. Spanos[4], Miltiadis I. Matsagkas[4], Athanasios D. Giannoukas[4], Christos G. Manopoulos[2], Efstratios E. Tzirtzilakis[5], Michalis A. Xenos[1]

[1]Department of Mathematics, University of Ioannina, Ioannina, 45110, Greece.

[2]Laboratory of Biofluid Mechanics & Biomedical Technology, School of Mechanical Engineering, National Technical University of Athens, Athens, Zografou 15772, Greece.

[3]Department of Vascular Surgery, Attikon University Hospital, National and Kapodistrian University of Athens, Athens, 10679, Greece.

[4]Department of Vascular Surgery, Faculty of Medicine, School of Health Sciences, University of Thessaly, Larissa, 41334, Greece.

[5]Department of Civil Engineering, University of the Peloponnese, Patras, 26334, Greece.

INTRODUCTION & AIM

- The Problem: Traditional clinical assessment relies on maximum diameter to predict AAA rupture risk, but this scalar metric fails to capture complex, patient-specific fluid dynamics.
- The Driver: Biomechanical research shows AAA progression is governed by Wall Shear Stress (WSS)—the frictional force exerted by blood flow on the endothelial lining.
- The Limitation: Standard hemodynamic metrics like TAWSS (Time-Averaged Wall Shear Stress) and OSI (Oscillatory Shear Index) lack the spatial resolution required to pinpoint exactly where near-wall flow becomes dysfunctional.

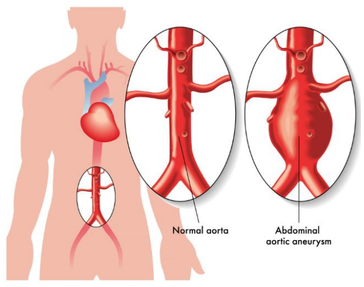

Figure 1: Medical illustration contrasting a normal abdominal aorta with a localized dilatation, or abdominal aortic aneurysm.

This study presents a high-fidelity computational framework comparing healthy and AAA hemodynamics by coupling 3D Navier-Stokes simulations with a 1D multiscale arterial network model to provide physiologically realistic boundary conditions. This work introduces a novel approach that treats wall shear stress as a dynamical system, employing Topological Skeleton Analysis to precisely identify fixed points where flow velocity vanishes, pinpointing critical stagnation and separation zones.

Jacobian eigenvalues are employed to detect unstable manifolds. Quantify the Topological Shear Variation Index (TSVI), a robust marker for recurring mechanical stimulation and endothelial cell permeability. By integrating these advanced topological indicators with classical CFD data, this research aims to provide a more nuanced understanding of the mechanical environment within aneurysms, potentially offering superior predictors for patient-specific rupture risk than diameter-based metrics alone.

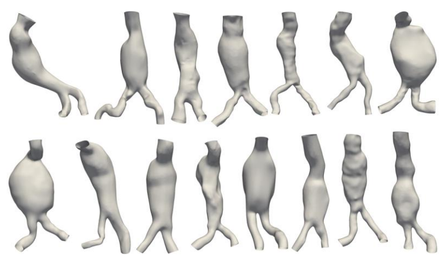

Figure 2: Three-dimensional anatomical reconstructions highlighting the diverse shapes and structural variations of abdominal aortic aneurysms across different patients.

METHOD

Blood flow is treated as an incompressible, Newtonian fluid governed by the 3D transient Navier-Stokes equations for conservation of mass and momentum. The fluid density is set to ρ = 1060 kg/m^3 and dynamic viscosity to μ = 0.004 Pa/s. All vascular boundaries are modeled as rigid walls. To capture true physiology, time-periodic, pulsatile inlet velocity profiles are prescribed from a systemic 1D arterial network model based on cross-sectionally averaged conservation laws.

$$\rho\left(\frac{\partial \mathbf{u}}{\partial t} + (\mathbf{u}\cdot\nabla)\mathbf{u}\right) = -\nabla p + \mu\nabla^2\mathbf{u}$$

$$\nabla\cdot\mathbf{u} = 0$$

$$\frac{\partial A}{\partial t} + \frac{\partial q}{\partial x} = 0$$

$$\frac{\partial q}{\partial t} + \frac{\partial}{\partial x}\left(\frac{q^2}{A}\right) + \frac{A}{\rho}\frac{\partial p}{\partial x} = -\frac{2\pi\nu}{\delta}\frac{q}{A}$$

$$p(x,t) - p_0 = \frac{4}{3}\frac{Eh}{r_0(x)}\left(1 - \sqrt{\frac{A_0(x)}{A(x,t)}}\right)$$

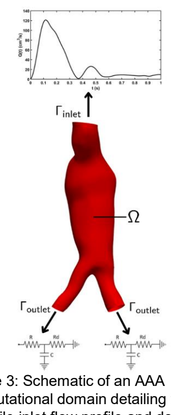

Figure 3: Schematic of an AAA computational domain detailing the pulsatile inlet flow profile and downstream RCR Windkessel models used for physiological outlet boundary conditions.

Outlets are coupled to three-element Windkessel (RCR) circuits tuned to match patient-specific target physiological pressures (120/80 mmHg). Simulations are discretized using stabilized linear finite elements via SVsolver and executed for 8 cardiac cycles to ensure complete periodic convergence (cycle-to-cycle variation <0.5%), utilizing the final cycle for post-processing.

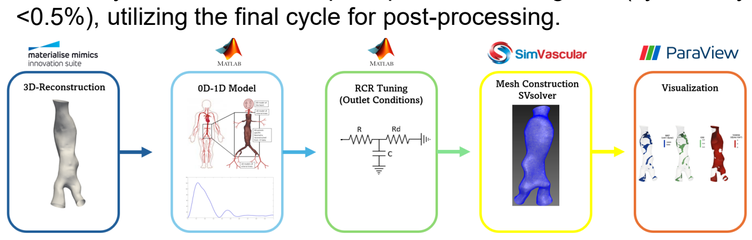

Figure 4: Schematic representation of the software pipeline and data workflow utilized for patient-specific modeling and simulation of an abdominal aortic aneurysm.

$$\mathrm{TAWSS} = \frac{1}{T}\int_0^T \|\tau_w(t)\|\,dt$$

$$\mathrm{OSI} = \frac{1}{2}\left(1 - \frac{\left\|\int_0^T \tau_w(t)\,dt\right\|}{\int_0^T \|\tau_w(t)\|\,dt}\right)$$

$$\mathrm{RRT} = \frac{1}{(1-2\,\mathrm{OSI})\,\mathrm{TAWSS}}$$

To quantify the near-wall physical environment before calculating the topological skeleton, standard Eulerian indicators are extracted from the finalized 8th cardiac cycle. TAWSS measures the average magnitude of frictional force on the wall. Critically low values (<4 dyne/cm^2) are linked to rapid aneurysm growth. OSI evaluates the directional change of WSS over the cycle. Values >0.3 denote highly unstable, multidirectional flow. RRT (Relative Residence Time): Highlights stagnation zones combining low shear and high oscillation, calculated directly from TAWSS and OSI. The critical risk cutoff is set at the 80th percentile cohort threshold (1.8349 cm^2/dyne).

The candidate fixed points are located precisely using the Poincaré Index on unstructured 3D meshes. They are subsequently classified into Saddles, Nodes (sources/sinks), or Foci using the local eigenvalues of the WSS Jacobian matrix to isolate zones of flow impingement and vortical separation. Finally, the mechanical stimulation experienced by the endothelial lining is enhanced by looking at structural stress variations over time.

Near-wall flow behavior is analyzed as a 2D dynamical system driven by the wall shear stress vector field. WSS fixed points are points where the WSS vector completely vanishes acting as the exact stagnation points of the near-wall flow.

$$TSVI(\mathbf{x}) = \left\{\frac{1}{T}\int_0^T \left[\nabla\cdot\tau_w(\mathbf{x},t) - \overline{\nabla\cdot\tau_w(\mathbf{x})}\right]^2 dt\right\}^{1/2}$$

$$\tau_w(\mathbf{x}) \approx J(\mathbf{x}^*)(\mathbf{x}-\mathbf{x}^*)$$

This index specifically computes the root-mean-square variability of WSS divergence over the full cardiac cycle, serving as a powerful indicator for predicting localized endothelial cell dysfunction and increased wall permeability.

RESULTS & DISCUSSION

Patient-specific CFD simulations showed clear hemodynamic differences between AAA and healthy aortas. AAA models exhibited larger regions of low TAWSS, elevated OSI, and high RRT, especially in the infrarenal aorta. These disturbed flow patterns were linked to flow recirculation, oscillatory motion, and prolonged particle residence, all associated with aneurysm progression and rupture risk.

Surface-based analysis demonstrated that AAA models exhibited markedly larger percentages of low TAWSS and high RRT regions compared to healthy controls. In the infrarenal region, the mean surface coverage of low TAWSS reached 57.96 ± 13.68% in AAA cases versus 25.30 ± 16.54% in healthy models, while RRT values were also substantially elevated (17.37 ± 8.17% vs 6.76 ± 5.00%).

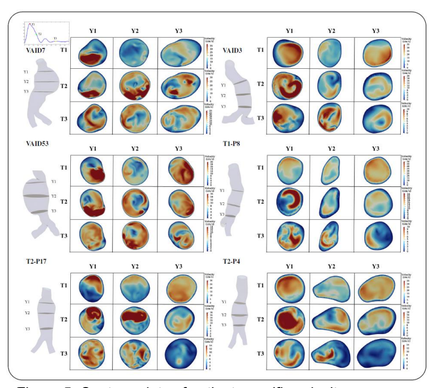

Figure 5: Contour plots of patient-specific velocity distributions inside abdominal aortic aneurysms, compared across three cross-sectional planes (Y1, Y2, Y3) and three specific phases of the cardiac cycle (T1, T2, T3).

Mean ± SD (%)	Infrarenal Region		Iliac Region	
	AAA	Healthy	AAA	Healthy
TAWSS	57.96 ± 13.68	25.30 ± 16.54	3.87 ± 3.59	1.17 ± 2.41
OSI	15.48 ± 7.76	11.55 ± 7.67	0.65 ± 0.47	0.33 ± 0.63
RRT	17.37 ± 8.17	6.76 ± 5.00	0.68 ± 0.77	0.11 ± 0.32

Table 1: Mean and standard deviation values of hemodynamic metrics (TAWSS, OSI, and RRT) within the infrarenal and iliac regions for AAA and healthy patient models.

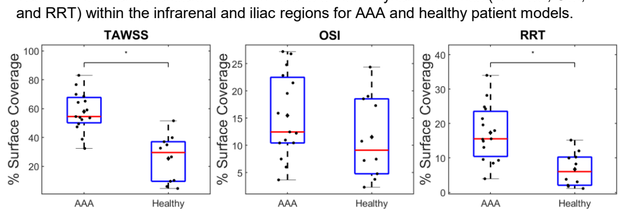

Figure 6: Boxplots comparing the percentage of surface coverage for TAWSS, OSI, and RRT between AAA and healthy cohorts, with individual patient distributions plotted as data points.

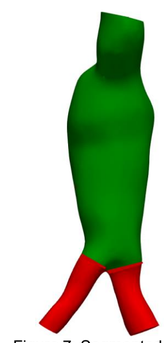

Figure 7: Segmented 3D model of an abdominal aortic aneurysm showing the isolated infrarenal aortic sac (green) and the iliac artery regions (red).

Although OSI increased in aneurysmal geometries, the differences were less pronounced, suggesting OSI alone may not fully capture disturbed hemodynamics. AAA models showed concentrated abnormal wall shear stress near aneurysm sacs and bifurcations, while healthy aortas exhibited more uniform, stable flow. Velocity slice visualizations further revealed pronounced vortex structures, flow separation, and asymmetric jet-like patterns during the cardiac cycle in AAA cases, indicating regions of recirculation and reduced flow stability. In contrast, healthy aortas maintained smoother and more organized velocity distributions.

Topological analysis of the WSS field identified saddle points, separation zones, and recirculation patterns that indicate unstable near-wall flow. Combining these topological features with CFD biomarkers offers a more comprehensive framework for AAA biomechanics, potentially improving rupture-risk assessment beyond maximum diameter alone. Within the aneurysmal sac, high TSVI regions near recirculation zones and complex vortical structures highlight strong temporal variations during the cardiac cycle. Ultimately, the increased complexity of the WSS topological skeleton marked by red fixed points and yellow saddle points directly quantifies disturbed flow organization and pronounced recirculation within AAA geometries.

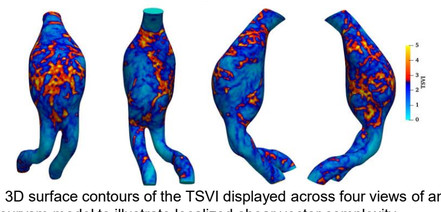

Figure 9: 3D surface contours of the TSVI displayed across four views of an abdominal aortic aneurysm model to illustrate localized shear vector complexity.

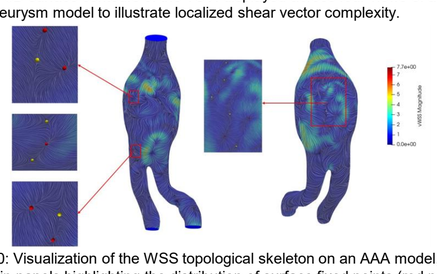

Figure 10: Visualization of the WSS topological skeleton on an AAA model, with zoomed-in panels highlighting the distribution of surface fixed points (red points) and saddle nodes (yellow color).

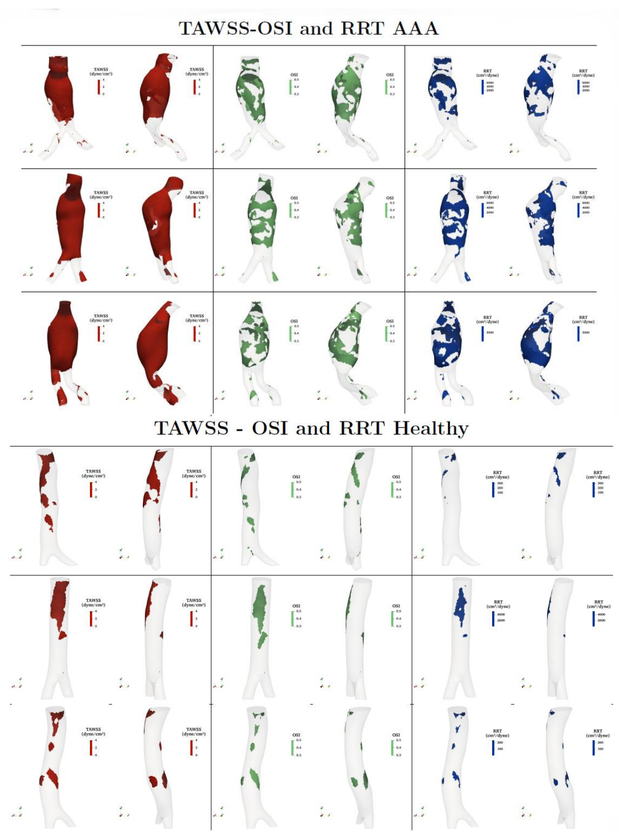

Figure 8: Comparative surface contour plots of TAWSS (red), OSI (green), and RRT (blue) between three AAA geometries and three healthy control models, showing both anterior and posterior views.

CONCLUSION

- Adverse Hemodynamics in AAA: Aneurysmal models exhibit significantly larger surface areas exposed to critically low TAWSS and high RRT compared to healthy aortas across both the infrarenal and iliac regions.
- OSI Insufficiency: The OSI alone is an insufficient standalone marker of disturbed flow and must always be interpreted in combination with TAWSS and RRT.
- TSVI successfully identifies structural flow variations, mapping localized zones of high endothelial cell mechanical stimulation and potential wall permeability.

REFERENCES

1. Katsoudas S, Linardopoulos P, Raptis A, et al. Hemodynamic Shear Stress Patterns in Abdominal Aortic Aneurysms and Healthy Aortas: A CFD Study. Cardiovasc Eng Technol. 2026.
2. Katsoudas S, Kyriakoudi K, Chrimatopoulos G, et al. Linking aneurysmal geometry and hemodynamics using computational fluid dynamics. Phys Fluids. 2026;38(3).
3. Mazzi V, Gallo D, Calò K, et al. A Eulerian method to analyze wall shear stress fixed points and manifolds in cardiovascular flows. Biomech Model Mechanobiol. 2020;19(4):1403–1423